

Original article

Numerical Modeling of the Black Sea Response to the Intrusion of Abnormally Cold Air in January 23–25, 2010

V. V. Efimov , D. A. Yarovaya

Marine Hydrophysical Institute of RAS, Sevastopol, Russian Federation
 *vefim38@mail.ru*

Abstract

Purpose. The work is aimed at studying the response of the Black Sea upper layer to the intrusion of cold air in January 23–25, 2010.

Methods and Results. The NOW coupled mesoscale sea – atmosphere model with the 1 km resolution was used to study the sea fields numerically. The change in sea surface temperature in January 23–25, 2010 resulted from the cold intrusion was reproduced. The basic factors which had influenced the change in the upper layer temperature, namely horizontal advection, cooling of the sea surface due to the sensible and latent heat fluxes and the impact of vertical turbulent mixing were considered and quantitatively assessed. The main changes that took place in the cold intermediate layer were investigated.

Conclusions. The change in vertical distribution of the monthly average temperature, salinity and density is considered based on the Copernicus reanalysis data for 2009–2010. The presence of a cold intermediate layer at the average depth 60 m in all the months except for the transitional winter-spring period is shown. The results of NOW modeling reveal the fact that decrease in the surface temperature over the most sea area occurred as a result of heat and mass exchange with the atmosphere. The influence of horizontal advection and mixing through the lower boundary of the cold intermediate layer was manifested only in certain small areas, in other words, it produced a local effect. Convective cooling spanned the upper mixed layer up to the depths about 40–45 m and amounted to ~ 1°C. Besides, it is shown that during the cold air intrusion, the depth of cold intermediate layer increased. The notion that the local cold waters in the shallow northwestern part of the sea are secondary as a source of formation of the cold intermediate layer has been confirmed. The density of colder, but less saline coastal water prevents its sinking to the upper boundary of cold intermediate layer.

Keywords: cooling, cold intermediate layer, mesoscale modeling, coupled model, sea surface temperature

Acknowledgments: The work was carried out within the framework of project FNNN-2024-0014 “Fundamental studies of interaction processes in the ocean-atmosphere system determining variability of physical state of marine environment at various spatiotemporal scales”.

For citation: Efimov, V.V. and Yarovaya, D.A., 2024. Numerical Modeling of the Black Sea Response to the Intrusion of Abnormally Cold Air in January 23–25, 2010. *Physical Oceanography*, 31(1), pp. 120-134.

© 2024, V. V. Efimov, D. A. Yarovaya

© 2024, Physical Oceanography

Introduction

Seasonal cooling of the Black Sea in the autumn-winter period is sometimes accompanied by episodes of sharp decreases in air temperature as a result of intrusions of cold air masses through the northern and northeastern boundaries of the region. Cold intrusions are usually associated with the formation of such an interesting and important feature of the sea thermohaline structure as cold intermediate layer (CIL): it is believed that the minimum water temperature at depths of 50–90 m is the result of deep convection of cold-water masses in winter in

the centers of cyclonic gyres [1]. This process is facilitated by the development of cyclonic circulation in the atmosphere above the sea leading to a water rise in the central regions of the sea, a decrease in the thickness of the upper mixed layer there and its more intense cooling¹ [2].

The second mechanism for the CIL development is considered to be the slope advection of cold water from the shallow northwestern part of the sea to the southwestern and further to the southern and southeastern coastal parts of the sea by the Rim Current (RC). In this case, part of these coastal cold waters is captured by mesoscale anticyclonic eddies in the Rim Current region and then spreads to the entire Black Sea region [1, 3–7].

The study of CIL formation mechanisms in the Black Sea has intensified in the last two decades. This was facilitated by the implementation of the ARGO ocean monitoring program which made it possible to supplement significantly the existing database of long-term, though rather scattered, data on shipboard measurements of temperature, velocity and salinity [8]. In addition, modern numerical models of circulation in the atmosphere – sea system provide the solution of the problem of reconstructing the thermohydrodynamic fields and their variability in a wide range of spatio-temporal scales [9, 10]. Without dwelling on a detailed analysis of the current state of knowledge of thermodynamic processes in the Black Sea and, in particular, the CIL formation, we note [11, 12] in this regard. In [11], a sea circulation modeling on a climatic time scale was carried out using realistic meteorological forcing and the above-mentioned idea about the mechanisms of CIL formation in the Black Sea was confirmed. In [12], the results of an analysis of the accumulated array of measurement data from subsurface buoys are presented; this made it possible to study the details of the CIL structure formation, its interannual variability and confirm the trend towards a decrease in its depth observed in the last decade.

As a rule, periods of cold air masses intrusion across the northern and northeastern boundaries of the region are associated with such extreme weather phenomena as the Novorossiysk bora [13], icing of roads in the steppe part and a significant decrease in air temperature in the usually warm region of the Southern Coast of Crimea. In practice, cold air intrusions are accompanied by cases of heavy fog over bays in coastal cities, disruption of ferry service and formation of characteristic cloud “tracks” in the atmosphere above the sea [14, 15]. At the same time, the reaction of the sea itself to these cases of intrusion has not been studied sufficiently.

One of such cases considered in this paper refers to January 23–25, 2010. Previously, we considered it in [14, 15] in order to study the convection rolls (two-dimensional convection) in the atmosphere using the WRF numerical atmospheric circulation model. The work is purposed at studying the reaction of the Black Sea upper layer to this cold air intrusion using a coupled model that makes it possible to reconstruct the interaction processes in the atmosphere – sea system numerically.

¹ Blatov, A.S., Bulgakov, N.P., Ivanov, V.A., Kosarev, A.N. and Tuljulkin, V.S., eds., 1984. *Variability of the Black Sea Hydrophysical Fields*. Leningrad: Gidrometeoizdat, 240 p. (in Russian).

Numerical model

NOW coupled model consists of well-known WRF atmospheric model, NEMO marine model latest version 4 and OASIS application that exchanges data between WRF and NEMO [16]. This model is described in more detail in our previous works [17, 18].

The modeling used two nested grids with a resolution of 3 and 1 km. Data exchange took place both between main and nested domains. Every two hours, sea surface temperature and surface current velocity are transmitted from NEMO to WRF and short-wave and long-wave radiative heat fluxes, sensible and latent heat fluxes, wind friction stress as well as the difference between evaporated moisture and precipitation are transmitted from WRF to NEMO. 37 vertical levels were applied in the atmospheric model and 75 – in the sea model.

Yonsei University Scheme was used to parameterize the planetary boundary layer in WRF. To parameterize vertical turbulent mixing in NEMO, the Generic Length Scale scheme was applied. Output interval of the modeling results was 1 hour. In WRF and NEMO, the modeling time step was 15 and 300 s, respectively, for a computational grid with a resolution of 3 km and 5 and 100 s for a grid with a resolution of 1 km. As in our previous work [18], the initial conditions for the marine model as well as the bottom topography were taken from the global Copernicus² reanalysis with a resolution of $1/12^\circ$ and the initial and boundary conditions for the atmospheric model were taken from ERA5 reanalysis. Since the Copernicus reanalysis is derived from NEMO model with observational data assimilation and sea surface atmospheric forcing taken from ERA5 reanalysis, this reduces significantly the time required to adapt NEMO and WRF to each other during the coupled modeling.

The calculation began at 00:00 on January 22, one day before the start of the intrusion episode which lasted about 4 days, and the total duration of modeling was 5 days. Due to the short duration of modeling, the river runoff effect was not taken into account in the marine model. In the atmospheric model in the computational domain with a resolution of 3 km we used spectral “nudging” – a method in which during the modeling the atmospheric fields are adjusted every six hours, i.e. “nudged” to the large-scale reanalysis fields.

Results and discussion

Features of the cold air intrusion episode

As a rule, the cold air intrusion into the Black Sea through the northern, northeastern boundaries develops on the southeastern periphery of the anticyclone with its center above the Baltic States [13]. Moreover, the duration of such intrusion episodes is relatively short and amounts to 2–4 days. The case we are considering lasted about 3 days, during which the strong northerly wind changed to northeasterly

² Copernicus Marine Service. *Global Ocean Physics Reanalysis*. [online] Available at: https://resources.marine.copernicus.eu/product-detail/global_multiyear_phy_001_030/information [Accessed: 20 February 2024].

with maximum velocities in the central and southwestern parts of the sea. Without considering the details of wind field variability during the entire intrusion episode, we give an example of wind speed variability at two points in the sea as well as the main forcing that determined the reaction of the sea – sensible heat fluxes, shf, and latent heat fluxes, lhf, through the surface (radiative fluxes in winter can be neglected for this period).

Fig. 1 shows wind speed values at a height of 10 m at two points in the northwestern and eastern parts of the sea. Fig. 2 demonstrates total heat flux from the surface averaged over the cold intrusion (January 23–25), shf + lhf. It is clearly seen that for the entire sea the episode under consideration can indeed be considered a three-day cold air intrusion. During this period, the sea cooling was heterogeneous: the western and eastern halves of the sea are separated by a small area of reduced fluxes which is naturally explained by a wind speed decrease behind the leeward slope of rather high Crimean Mountains [13]. At the same time, heat loss from the surface in the northern part of the sea was 500–600 W/m², wind speed was about 10–14 m/s. In the southern half of the sea, heat loss through the surface is smaller than in the northern half since cold air warmed up when moving above a warmer sea.

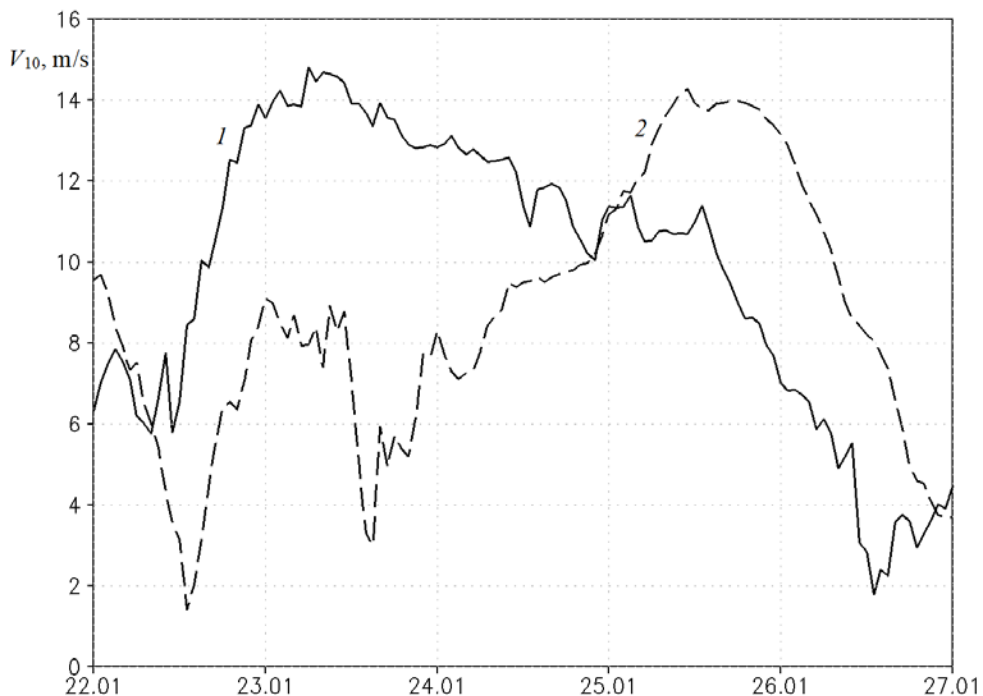


Fig. 1. Surface wind speed, m/s, at the points with coordinates 31°E, 44.5°N (1) and 37.5°E, 43°N (2) in January 22–26, 2010. The point positions are shown in Fig. 2

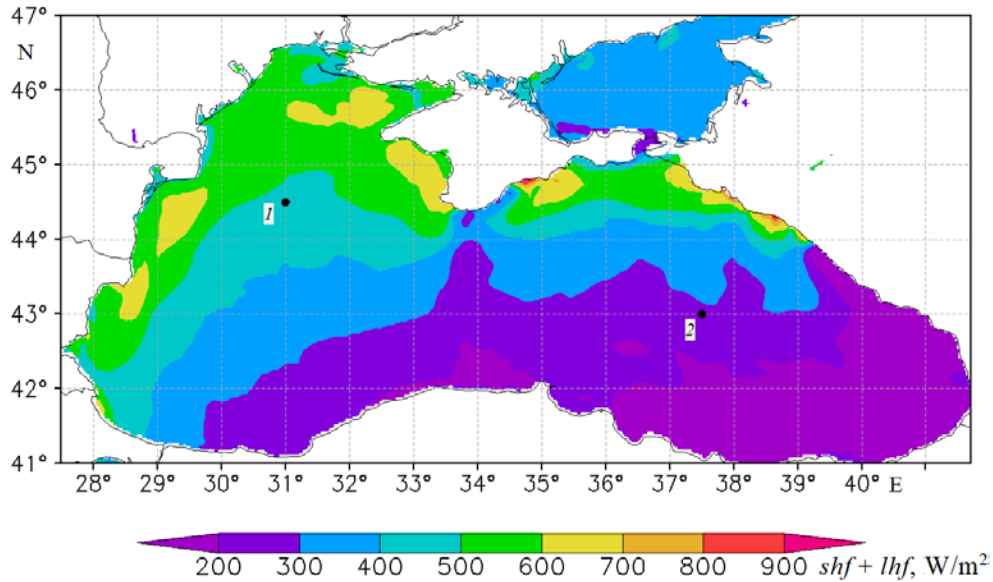


Fig. 2. Total heat flux directed from the sea surface, W/m^2 , averaged for January 23–25, 2010

Changes in sea surface temperature

Fig. 3, *a* shows the distribution of sea surface temperature (SST) and surface current velocity at the beginning of the cold invasion. A well-known climatic feature of the SST distribution – increased temperature values in the southeastern part and decreased in the northwestern one and Rim Current along the entire boundary area of the sea – is presented well. Fig. 3, *b* demonstrates the SST variations for the entire period of intrusion, from 00:00 on January 23 to 00:00 on January 26. As expected, the SST decrease is heterogeneous in area reflecting both synoptic heterogeneity of atmospheric forcing and mesoscale structure of eddy and jet currents in the sea upper layer. On average, the SST decreased during the intrusion by $1.5\text{ }^\circ\text{C}$ (in the deep sea) and even more in the coastal region of the northwestern shelf, where heat loss from the surface reached $500\text{--}600\text{ W/m}^2$. A comparison of current velocity fields immediately before and after the cold intrusion showed that on January 23–25 the Rim Current intensity increased, and in some areas near the Crimean coast, in the southwestern and southeastern corners of the sea, the velocity of alongshore surface current increased by $\sim 0.2\text{ m/s}$.

The SST decrease during winter cooling is determined by turbulence in the upper mixed layer, thickness of the upper mixed layer (UML) and advective heat transfer. All these processes are reproduced in detail in NEMO.

Fig. 3, *c – e* shows separately the contribution of the main factors to the SST variation: a decrease in the SST due to sensible and latent heat fluxes from the sea surface ΔT_{hf} (Fig. 3, *c*), the SST variation due to horizontal advection ΔT_{adv} (Fig. 3, *d*) and vertical turbulent mixing ΔT_{dif} (Fig. 3, *e*). The values given in Fig. 3, *c – e* are calculated using the following simple formulas:

$$\Delta T_{hf} = \frac{(shf + lhf)}{\rho C_p H} \Delta t, \quad (1)$$

$$\Delta T_{adv} = -\Delta t \int_{-H}^0 \left(u \frac{\partial T}{\partial x} + v \frac{\partial T}{\partial y} \right) dz, \quad (2)$$

$$\Delta T_{dif} = -\frac{\Delta t}{H} \left(K \frac{\partial T}{\partial z} \right) \Big|_{z=-H}, \quad (3)$$

where H is UML thickness; T is water temperature; u and v are zonal and meridional current velocities; K is coefficient of vertical turbulent heat diffusion (calculated in the model); ρ and C_p are density and specific heat capacity of water; Δt is time period (equal to 1 h). The details of numerical calculation by these formulas are given in [17]. H value in formulas (1)–(3) was assumed to be equal to the upper layer thickness with small (< 0.02 °C/m) vertical gradient T or to the sea depth if the water temperature at a given point does not almost vary with depth (near the coast and in the Sea of Azov).

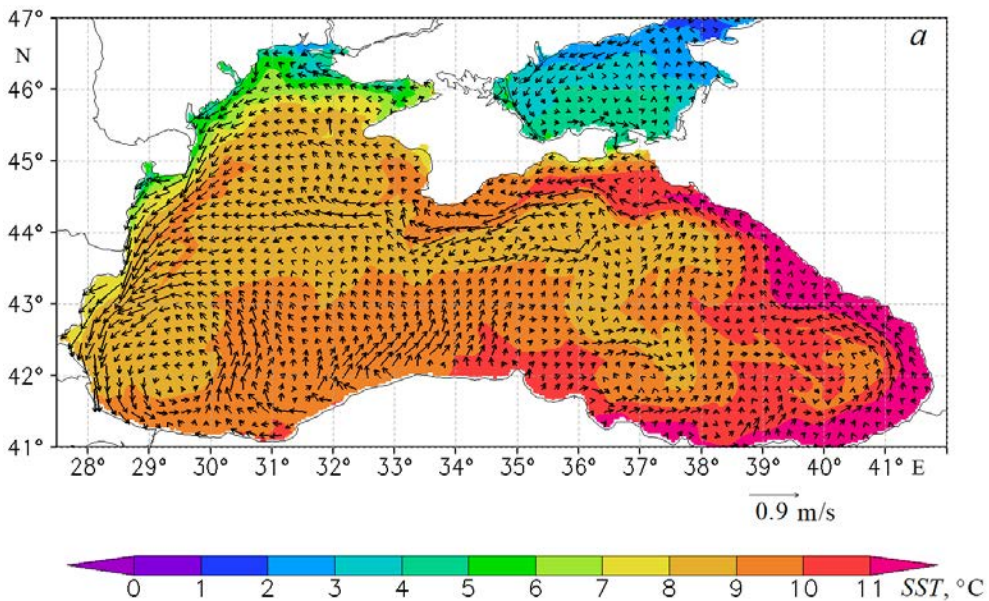
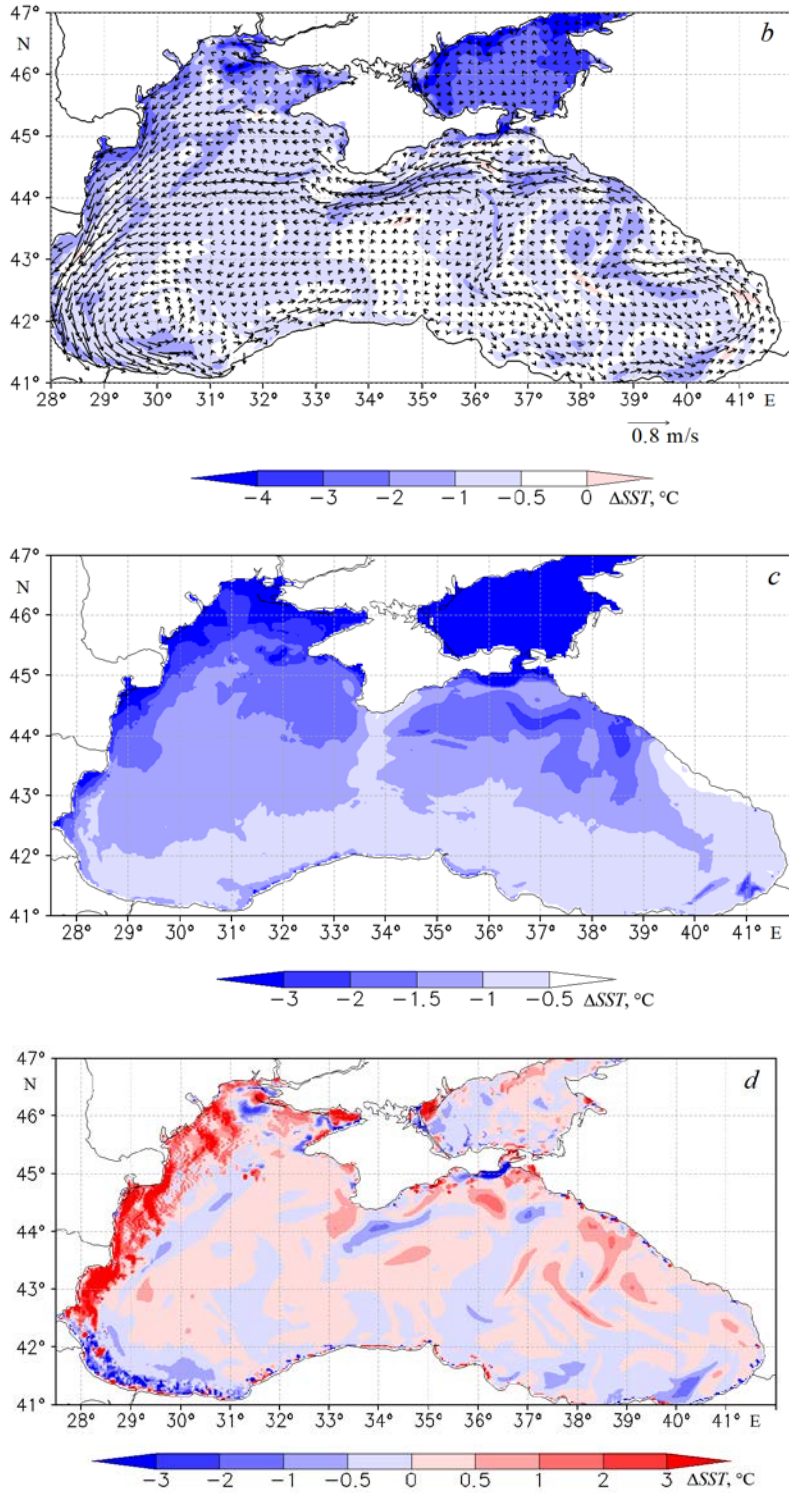
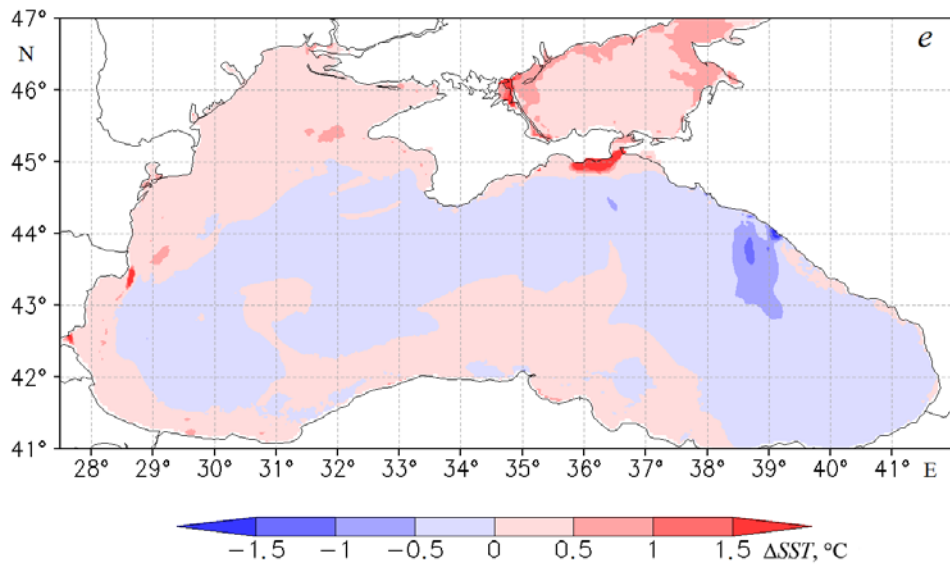


Fig. 3. Sea surface temperature (SST) at 00:00 on January 23 (*a*); change of SST for the period from 00:00, January 23, to 00:00, January 26, based on the results of modeling (*b*) and calculation using formulas (1) (*c*), (2) (*d*) and (3) (*e*). Arrows show the current velocity on the surface (m/s) at 00:00, January 23 (*a*), and the average one for the period from 00:00, January 23, to 00:00, January 26 (*b*). For clarity, the number of arrows is reduced along the longitude and latitude with the increments 15 and 12, respectively



Continuation of Fig. 3.



Continuation of Fig. 3.

Fig. 3, *c* shows the SST variation during the cold intrusion period due to heat fluxes. A significant SST decrease in the northern part of the sea is associated not only with high surface wind speed there, but also with shallow depths. Fig. 3, *c* distinguishes the region stretching from the Crimea to the south and the region near the Caucasian coast, eastwards of 39°E, where $|\Delta T_{\text{hf}}|$ value is smaller than in the deep sea. This is obviously due to the effect of the coastal Crimean and Caucasus mountains. Without providing illustrations, we note that in the atmospheric model, in the surface wind field averaged over January 23–25, qualitatively similar local features are observed – an area with reduced wind speed in the central part of the sea southwards of Crimea and low-velocity area near the high-mountainous Caucasian coast.

Fig. 3, *d* demonstrates temperature decrease averaged over depth H due to the horizontal transport of cold waters in the sea upper layer. As can be seen from Fig. 3, *b*, an area of the reduced SST arose southwards of Crimea despite the relatively small heat flux from the sea surface. Fig. 3, *d* shows that this occurred due to the transfer of cold waters from the northeastern part where heat exchange with the atmosphere was stronger, and as a result cooling was stronger as well. The Rim Current velocity increases as it goes around the Crimean Peninsula (Fig. 3, *a*) and, as a consequence, horizontal advection effect on the SST in this place increases. The advective Rim Current effect on the SST field is also manifested near the western coast where warmer water is transported from the central part of the sea and near the southwestern coast where colder water is transported from the northwestern part (Fig. 3, *b*). Note that the vertical transport effect on the SST field variation was insignificant and is not reflected in the figures.

As can be seen from Fig. 3, *e*, except for a small area near the Caucasian coast, the vertical mixing effect on the SST in the deep part of the sea was relatively small.

In the shallow part of the sea, e.g. near the Kerch Peninsula, owing to sharp sea surface cooling, convective instability could lead to the SST increase due to temperature equalization in the entire layer down to the bottom.

Thus, the Black Sea response to the cold intrusion consisted of the SST decrease mainly by 1–2 °C under effect of large sensible and latent heat fluxes (Fig. 3, *c*). The effect of horizontal advection (Fig. 3, *d*) and vertical turbulent mixing (Fig. 3, *e*) on the SST, as expected, led only to local inhomogeneities in the temperature field.

Changes in the sea upper layer temperature

As mentioned in the introduction, a characteristic feature of temperature distribution in the Black Sea upper layer is CIL – a relatively thin intermediate layer between the thermo- and halocline at depths of about 60 m. The current state of knowledge on the CIL is presented well in [12].

Fig. 4, *a, b* shows the vertical structure of temperature, salinity and density fields at vertical sections drawn along 31°E and 44°N before the start of the cold intrusion. Fig. 4, *a, b* confirms the idea that local cold waters in the shallow northwestern part of the sea are secondary as a source of CIL formation. Indeed, neither Fig. 4, *a, b*, nor other zonal and meridional vertical sections demonstrate signs of cold waters propagation from the coast towards the open part of the sea. The density of colder, though less saline, coastal water prevents it from sinking to the upper boundary of CIL, and its isolation from CIL is clearly visible.

The pattern of fields at vertical sections confirms the idea of CIL presence throughout the entire sea area except for certain local areas associated with coastal orography, river mouths and circulation features¹. Fig. 4, *b* demonstrates clearly the rise of CIL following the rise of UML and thermocline in the central part of the sea as a result of development of large-scale cyclonic circulation and the Rim Current [1]. Local deepening of CIL in the area of 33°–34°E is associated with a local effect – the proximity of the Southern Coast of Crimea which affects the Rim Current displacement and creates meridional heterogeneity of the density and temperature fields. Consideration of the features of CIL distribution throughout the sea as well as taking into account the CIL interannual temporal variability and its disappearance in individual years is beyond the scope of the work since the circulation was reproduced only for a relatively short time interval of the cold intrusion.

In Fig. 4, *c*, temperature and salinity variations during the cold intrusion are given at the same vertical section as in Fig. 4, *b*. In the near-surface layer, water cooling by up to 1.5–2 °C is clearly visible; this corresponds to the SST decrease in Fig. 3, *b*. In the CIL layer and below, the temperature varied insignificantly from –0.5 to 0.5 °C. To distinguish such a small reaction of the CIL temperature, we constructed vertical temperature profiles averaged over a large area (30°–38°E, 42.5°–44°N) and considered the period of cold intrusion in the annual cycle of CIL variation for 2009–2010.

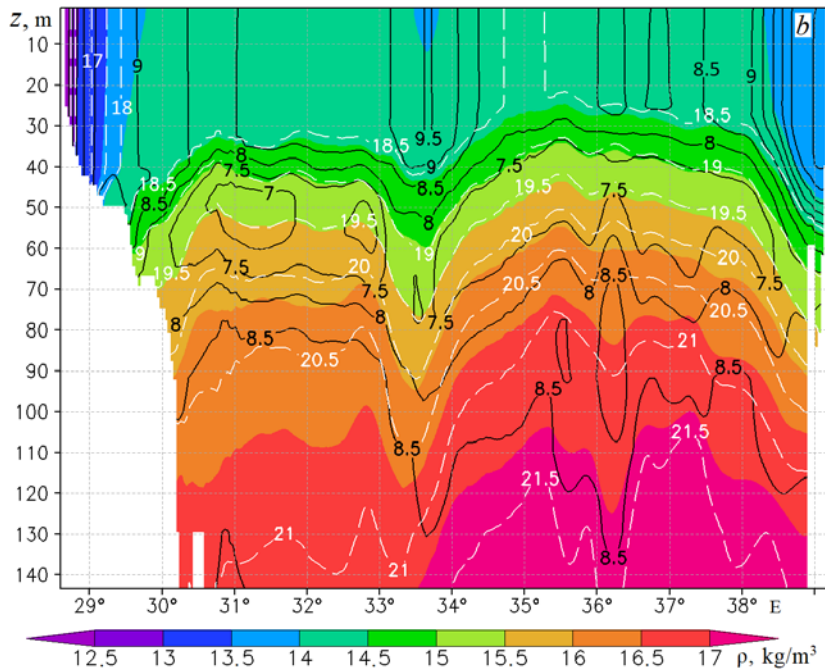
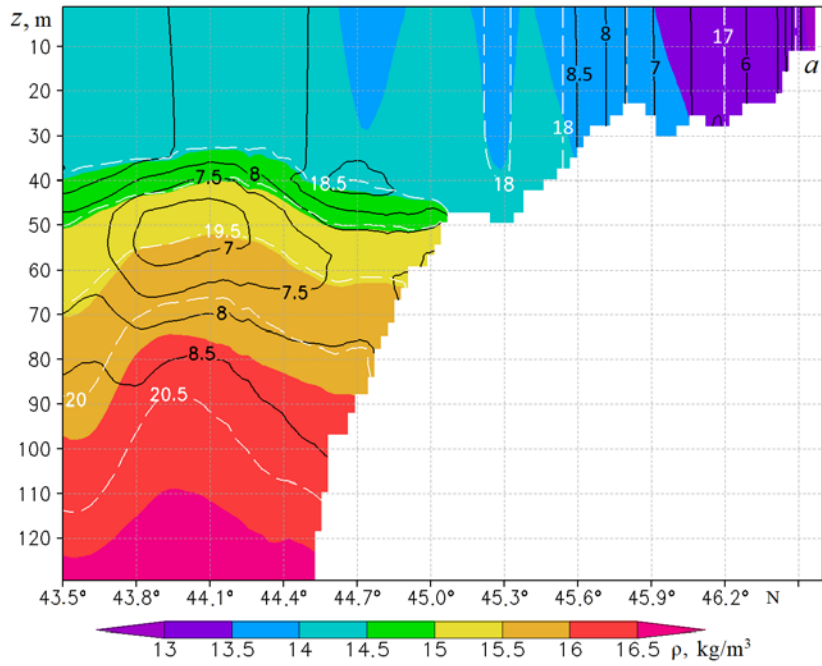
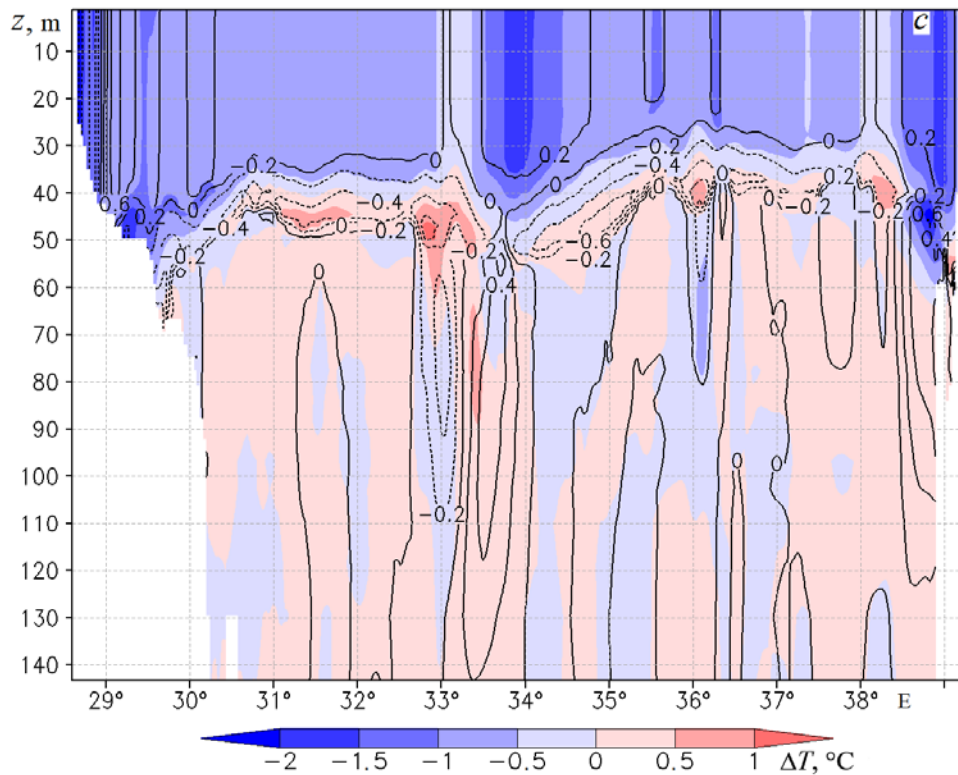


Fig. 4. Fields of density ρ , kg/m^3 , temperature T , $^\circ\text{C}$ (black isolines), and salinity S , ‰ (white isolines), at 00:00, January 23, at the meridional section along 31°E (*a*) and the zonal section along 44°N (*b*); change in temperature, $^\circ\text{C}$, and salinity, ‰ (isolines), for the period from 00:00, January 23, to 00:00, January 26, at the section along 44°N (*c*). For clarity, not the very value of ρ , but the difference ($\rho - 1000$), kg/m^3 , is shown in Fig. 4, *a*, *b*



Continuation of Fig. 4

Fig. 5 shows vertical profiles of temperature, density, and salinity averaged over the deep-sea part for several months of 2009–2010 and constructed using Copernicus data set. As can be seen, our cold intrusion episode occurred in mid-winter, when seasonal cooling brought the upper seasonal thermocline close to disappearing, although with the existence of CIL. Without dwelling on the features of seasonal variations in the vertical profiles of the main hydrophysical characteristics in the sea upper layer, we will only note well-pronounced temperature fluctuations in the annual cycle, a salinity decrease in summer in the upper layer associated with increased evaporation and a corresponding decrease in density. No deviations from the monotonic decrease in density and salinity were observed in the entire upper layer from August 2009 to February 2010. In all seasons except for the transitional winter-spring season we observe CIL with a minimum temperature value at an average depth of 60 m in the temperature profiles for our annual period of 2009–2010.

Taking into account that the cold air intrusion occurred when the sea upper layer had almost completely cooled, we will consider in more detail the development of this process according to our modeling results in which CIL was reproduced with a fairly high vertical resolution of ~ 2 m. Note that vertical resolution in Copernicus data set is about 5 m which smoothes out small-scale features of temperature profile variations in CIL.

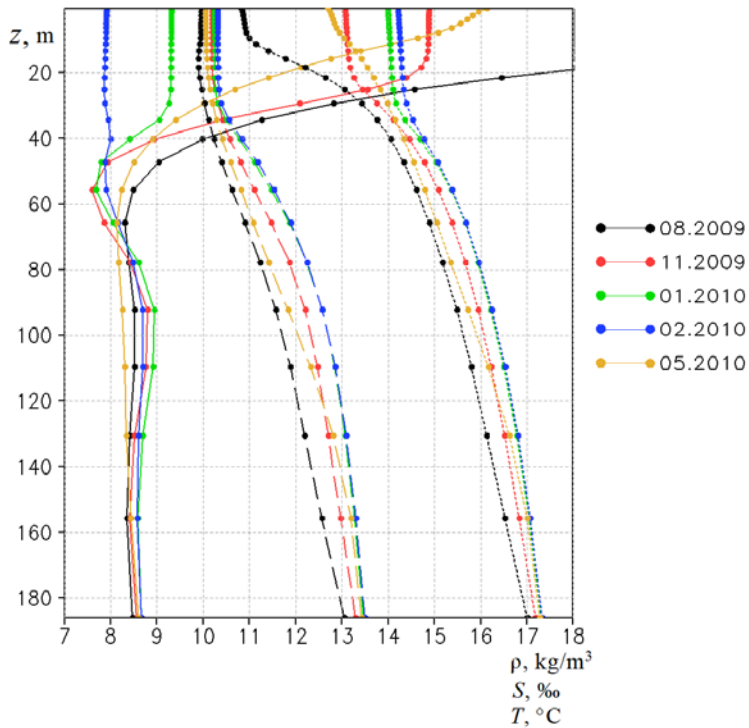


Fig. 5. Averaged over the deep-sea part (30° – 38° E, 42.5° – 44° N) monthly average vertical profiles of temperature T , $^{\circ}$ C (solid line), salinity S , ‰ (dashed line), and density ρ , kg/m^3 (dotted line), based on the Copernicus reanalysis data. For clarity, not the very values of S and ρ , but the differences ($S - 8$), ‰, and ($\rho - 1000$), kg/m^3 , are shown

Fig. 6 shows temperature and salinity profiles before, during and after the cold intrusion episode. The temperature field reaction is clearly visible: over 3 days the temperature of the entire upper layer decreased by $\sim 1^{\circ}\text{C}$ – this is consistent with the SST decrease shown in Fig. 3, *b*. It is interesting to note that the temperature decrease at the CIL upper boundary has a characteristic feature known for the UML evolution in the summer-autumn period – the entrainment of water from the seasonal thermocline into the UML associated with the penetration of turbulent pulsations from the UML into the thermocline.

It can be clearly seen from Fig. 6 that temperature decrease and salinity increase are accompanied by deepening of the CIL upper boundary. As a rule, summer mixed layer occurs as a result of dynamic instability associated with wind stress at the sea surface and wave orbital motions. In our case, they do not penetrate to depths of more than 30–40 m and shear instability effects associated with thermohaline currents can probably be also neglected. Unlike the summer mixed layer, the turbulence in our case is of a convective nature and the entrainment is limited to the region of the CIL upper boundary. Fig. 6 shows that in the CIL and below both temperature and salinity profiles can be considered unchanged during the intrusion period. This indicates directly the smallness of dissipative effects at these depths which explains the long lifetime of CIL after its development during winter convection.

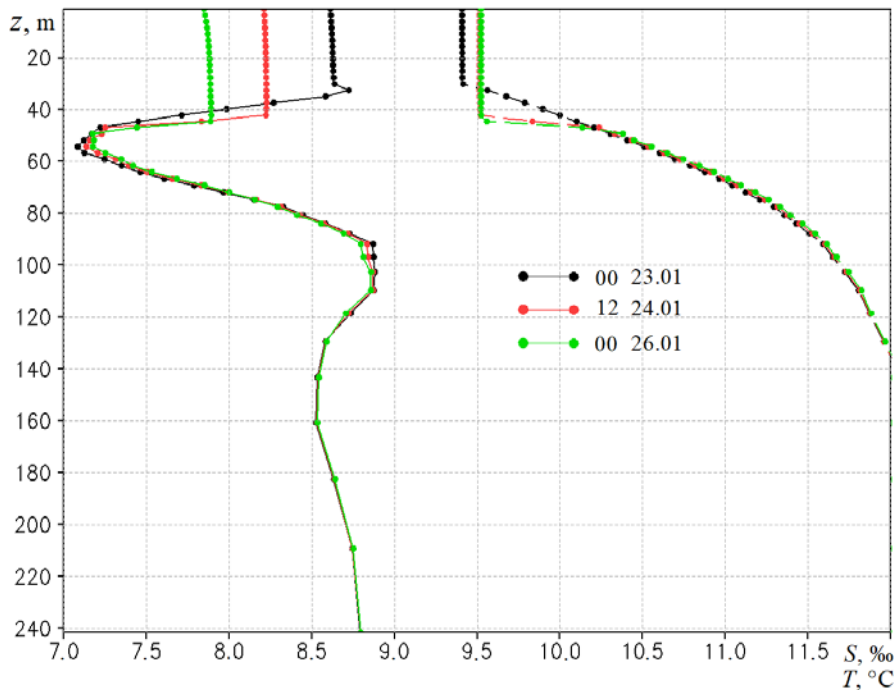


Fig. 6. Vertical profiles of temperature T , °C (solid line), and salinity S , ‰ (dashed line), at the point with coordinates 32°E, 44°N at 00:00 on January 23, 12:00 on January 24 and 00:00 on January 26, 2010. For clarity, not the very value of S , but the difference $(S - 8)$, ‰, is shown

Conclusion

Numerical modeling of the extreme case of cold air intrusion into the Black Sea using the coupled WRF-NEMO model with regard to the atmosphere-sea interaction made it possible to calculate the structure of thermohydrodynamic fields with a horizontal spatial resolution of 1 km. The intrusion itself lasted about three days during which wind speed reached 15 m/s and the total flux of sensible and latent heat was about 500 W/m^2 . The reaction of the sea directly to this cold atmospheric intrusion was distinguished. It was demonstrated that convective cooling influenced the upper mixed layer to the depths of about 40–45 m and amounted to $\sim 1 \text{ }^\circ\text{C}$.

It was demonstrated that the SST decrease over most sea occurred as a result of heat and mass exchange with the atmosphere. The effect of horizontal transport and vertical turbulent mixing on the SST appeared only in certain small areas, i.e. it had a local effect.

The case under study is of interest because it falls on the final lifetime stage of previously formed CIL: deepening of the CIL upper boundary (defined by the level of $8 \text{ }^\circ\text{C}$) due to autumn-winter cooling from the surface ended up with the example we considered. This is illustrated well by the temperature and salinity vertical profiles at the final stage of CIL lifetime as an intermediate layer between the thermo- and halocline. Small values of vertical diffusion and viscosity coefficients in CIL indicating the smallness of dissipative processes represent a characteristic feature.

CIL spatial distribution over the sea area is uneven. Nevertheless, in our case local areas of CIL absence are quite limited. At least, the given latitudinal section across the entire sea area and other sections (not presented here) do not manifest its development only in rare coastal areas. The corresponding climate analysis of CIL spatio-temporal structures as well as the statistics of cold intrusion cases in the Black Sea region (similar to the previously obtained statistics of Novorossiysk bora cases) are beyond the scope of this work and are proposed for the future.

REFERENCES

1. Korotaev, G.K., Knysh, V.V. and Kubryakov, A.I., 2014. Study of Formation Process of Cold Intermediate Layer Based on Reanalysis of Black Sea Hydrophysical Fields for 1971-1993. *Izvestiya, Atmospheric and Oceanic Physics*, 50(1), pp. 35-48. doi:10.1134/S0001433813060108
2. Simonov, A.I., Ryabinina, A.I. and Gershanovich, D.E., eds., 1992. *Hydrometeorology and Hydrochemistry of Seas in the USSR. Vol. IV. Black Sea. Issue 2. [Hydrochemical Conditions and Oceanographic Basis of Formation of Biological Productivity]*. Saint-Petersburg: Gidrometoizdat, 219 p. (in Russian).
3. Ivanov, V.A. and Belokopytov, V.N., 2013. *Oceanography of the Black Sea*. Sevastopol: ECOSI-Gidrofizika, 210 p.
4. Kuklev, S.B., Zatsepin, A.G. and Podymov, O.I., 2019. Formation of the Cold Intermediate Layer in the Shelf-Slope Northeastern Part Zone of the Black Sea. *Journal of Oceanological Research*, 47(3), pp. 58-71. doi:10.29006/1564-2291.JOR-2019.47(3).5 (in Russian).
5. Ovchinnikov, I.M. and Popov, Yu.I., 1987. Cold Intermediate Layer Formation in the Black Sea. *Oceanology*, 27(5), pp. 739-746 (in Russian).
6. Piotukh, V.B., Zatsepin, A.G., Kazmin, A.S. and Yakubenko, V.G., 2011. Impact of the Winter Cooling on the Variability of the Thermohaline Characteristics of the Active Layer in the Black Sea. *Oceanology*, 51(2), pp. 221-230. doi:10.1134/S0001437011020123
7. Titov, V.B., 2006. Zones of the Cold Intermediate Layer Formation and the Volume of Waters in the Black Sea Depending on Winter Severity. *Meteorologiya i Gidrologiya*, (6), pp. 62-68 (in Russian).
8. Akpinar, A., Fach, B.A. and Oguz, T., 2017. Observing the Subsurface Thermal Signature of the Black Sea Cold Intermediate Layer with Argo Profiling Floats. *Deep-Sea Research Part I: Oceanographic Research Papers*, 124, pp. 140-152. doi:10.1016/j.dsr.2017.04.002
9. Bruciaferri, D., Shapiro, G.I. and Wobus, F., 2018. A Multi-Envelope Vertical Coordinate System for Numerical Ocean Modelling. *Ocean Dynamics*, 68(10), pp. 1239-1258. doi:10.1007/s10236-018-1189-x
10. Bruciaferri, D., Shapiro, G., Stanichny, S., Zatsepin, A., Ezer, T., Wobus, F., Francis, X. and Hilton, D., 2020. The Development of a 3D Computational Mesh to Improve the Representation of Dynamic Processes: The Black Sea Test Case. *Ocean Modelling*, 146, 101534. doi:10.1016/j.ocemod.2019.101534
11. Miladinova, S., Stips, A., Garcia-Gorritz, E. and Macias, M.D., 2018. Formation and Changes of the Black Sea Cold Intermediate Layer. *Progress in Oceanography*, 167, pp. 11-23. doi:10.1016/j.pocean.2018.07.002
12. Stanev, E.V., Peneva, E. and Chtirkova, B., 2019. Climate Change and Regional Ocean Water Mass Disappearance: Case of the Black Sea. *Journal of Geophysical Research: Oceans*, 124(7), pp. 4803-4819. doi:10.1029/2019JC015076
13. Efimov, V.V., Komarovskaya, O.I. and Bayankina, T.M., 2019. Temporal Characteristics and Synoptic Conditions of Extreme Bora Formation in Novorossiysk. *Physical Oceanography*, 26(5), pp. 361-373. doi:10.22449/1573-160X-2019-5-361-373
14. Efimov, V.V. and Yarovaya, D.A., 2014. Numerical Simulation of Air Convection in the Atmosphere during the Invasion of Cold Air over the Black Sea. *Izvestiya, Atmospheric and Oceanic Physics*, 50(6), pp. 610-620. doi:10.1134/S0001433814060073

15. Iarovaia, D.A. and Efimov, V.V., 2018. Cloud Cells by Data of Satellite Measurements and Convective Energy Balance on Invasion of Cold Air into the Atmosphere over the Black Sea. *Izvestiya, Atmospheric and Oceanic Physics*, 54(9), pp. 1214-1222. doi:10.1134/S000143381809044X
16. Samson, G., Masson, S., Lengaigne, M., Keerthi, M.G., Vialard, J., Pous, S., Madec, G., Jourdain, N.C., Jullien, S. [et al.], 2014. The NOW Regional Coupled Model: Application to the Tropical Indian Ocean Climate and Tropical Cyclone Activity. *Journal of Advances in Modeling Earth Systems*, 6(3), pp. 700-722. doi:10.1002/2014MS000324
17. Iarovaia, D.A. and Efimov, V.V., 2021. Development of Cold Sea Surface Temperature Anomalies in the Black Sea. *Izvestiya, Atmospheric and Oceanic Physics*, 57(4), pp. 413-424. doi:10.1134/S0001433821040228
18. Efimov, V.V., Iarovaya, D.A. and Barabanov, V.S., 2023. Numerical Modelling of Upwelling near the South Coast of Crimea on 24–25 September 2013. *Ecological Safety of Coastal and Shelf Zones of Sea*, (1), pp. 6-19. doi:10.29039/2413-5577-2023-1-6-19

Submitted 19.04.2023; approved after review 22.05.2023;
accepted for publication 15.11.2023.

About the authors:

Vladimir V. Efimov, Head of Atmosphere and Ocean Interaction Department, Marine Hydrophysical Institute of RAS (2 Kapitanskaya Str., Sevastopol, 299011, Russian Federation), DSc (Phys.-Math.), Professor, **ResearcherID: P-2063-2017**, **Scopus Author ID: 6602381894**, vefim38@mail.ru

Daria A. Yarovaya, Senior Research Associate, Marine Hydrophysical Institute of RAS (2 Kapitanskaya Str., Sevastopol, 299011, Russian Federation), CSc (Phys.-Math.), **ResearcherID: Q-4144-2016**, **ORCID ID: 0000-0003-0949-2040**, **Scopus Author ID: 57205741734**, darik777@mhi-ras.ru

Contribution of the co-authors:

Vladimir V. Efimov – problem statement, discussion of modeling results, formulation of conclusions

Daria A. Yarovaya – carrying out calculations, discussion of modeling results, participating in drawing conclusions

The authors have read and approved the final manuscript.

The authors declare that they have no conflict of interest.